Magnetomechanical damping in stress-relieved Ni: the effect of the dc magnetic field

2008 J. Phys.: Condens. Matter 20 325227

(http://iopscience.iop.org/0953-8984/20/32/325227)

J. Phys.: Condens. Matter **20** (2008) 325227 (9pp) doi:10.1088/0953-8984/20/32/325227

Magnetomechanical damping in stress-relieved Ni: the effect of the dc magnetic field

A Ercuta

Faculty of Physics, West University, 300223 Timisoara, Romania

E-mail: ercuta@physics.uvt.ro

Received 19 March 2008, in final form 19 June 2008
Published 18 July 2008
Online at stacks.iop.org/JPhysCM/20/325227

Abstract

The effect of the dc magnetic field on the damping behaviour of a stress-relieved Ni sample is examined under low frequency free torsional vibrations. High damping capacity, reaching 40% fractional energy dissipation per full period was detected in stages of high magnetization, beyond 90% from technical saturation. The damping of magnetic origin is attributed to the vibration-induced movement of the still existing non-180° domain walls, through the irregular energy landscape generated by their interaction with the structure defects. The overall energy loss per full period of vibration is evaluated as the statistical addition of contributions from local dissipative processes consisting in forward and reverse Barkhausen jumps, triggered by the periodic stress and either favoured or suppressed by the field, depending on its strength. Predictions were obtained in good agreement with the experiment.

1. Introduction

Internal friction (IF) is the traditional term for the capacity of materials to attenuate vibrations; in solids this property is attributed to a large palette of microstructural mechanisms, among which point defect relaxation, dislocation relaxation, grain boundary relaxation, anelastic relaxation during phase transformations or thermo-elastic relaxation are widely studied [1, 2]. As a quantitative expression of the damping capacity, the fractional energy loss per full period of vibration [3, 4]:

$$D = \frac{\Delta W}{W_e} \tag{1.1}$$

is commonly used; here, ΔW is the energy lost per cycle at the expense of the elastic energy W_e stored at maximum strain. Alternatively, the reciprocal $Q^{-1} = D/2\pi$ of the quality factor (by analogy with ac circuits), the relative width at half power of the resonance curve, or the logarithmic decrement of the amplitude are sometimes preferred [2, 5].

Magnetostrictive materials exhibit a specific contribution to the damping, called 'magnetomechanical damping' (MMD) which originates in the dissipative processes that accompany the periodic changes (either microscopic or macroscopic) induced in their magnetic state by the applied stress [4–6]. It was found that in addition to the common vibration conditions like amplitude, frequency, temperature or loading mode, etc, the energy ΔW_m lost per cycle via such changes also depends on the strength and direction of the applied magnetic field [4, 6, 7a, 8]. As ΔW_m vanishes at magnetic saturation, in which case only a non-magnetic background damping, (D_{sat}), is observed, the MMD coefficient:

$$D_m = \frac{\Delta W_m}{W_e} \tag{1.2}$$

is currently evaluated by subtracting D_{sat} from the as-measured total damping. It was found that the MMD is practically frequency independent up to the kHz range, and that this is in a direct relation to a hysteresis effect observed in the stress–strain cycle of these materials, well below the conventional limits for plastic deformation [9–11]; the resulting area of the stress–strain loop was interpreted as the volume density of ΔW_m [7a, 12, 13, 14]. This damping mechanism is attributed to the vibration-driven irreversible jumps (Barkhausen jumps) of non-180° DWs, as they move through the irregular energy landscape generated by their interaction with structure defects (such as dislocations, slip traces, grain boundaries, non-magnetic inclusions, etc, [15, 16]). As a general feature, the MMD due to hysteresis depends on the amplitude of vibration [3, 17–21] and on the strength of the applied magnetic field [12, 14, 22], D_m showing a maximum in

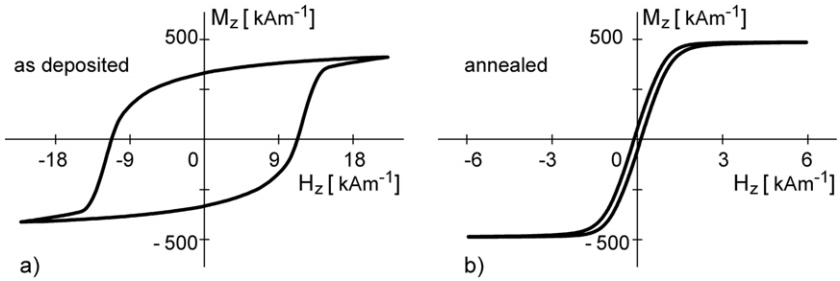

Figure 1. Hysteresis loops of the sample (a) in the native state and (b) after structural relaxation; the driving field H_z was applied longitudinally.

both cases. In addition, forced vibration experiments have shown that the amplitude dependence of the MMD exhibits hysteresis [4, 8]: below a 'critical' amplitude value (close to that at which D_m is maximum), the damping depends on whether the amplitude is increased or decreased, always being stronger in the latter case. Once a cycle (from zero to a preset maximum strain and back to zero) is completed for the first time, the hysteresis disappears, but it reappears if the amplitude is increased beyond the previous range. The effect was attributed to the fact that as the amplitude is increased, an increasing number of non-180° DWs are driven behind higher and higher internal stress peaks, thus settling back into some more stable sites [4, 23]. Since such 'trapping sites' are expected more in regions of higher density of structure defects, the movement of the DWs here will involve forward and reverse Barkhausen jumps, until the amplitude of vibration falls down below some local threshold-like values.

The irregular energy landscape through which the DW moves is often described by a random profile function. Sometimes called 'potential function' [24], the concept was introduced in the literature in various (in fact, equivalent) forms. Thus, in terms of the 'difference in the energy density of the dipoles on the two sides of the DW', Becker and Dörring [7b] interpreted the effect of the internal stresses on the initial susceptibility, while Bates [25] discussed the magnetic hysteresis. Alternatively, Néel [26] and other authors [27, 28] used the 'DW energy gradient' to express the DW contributions to the linear and quadratic Rayleigh terms. The influence of the internal stresses on the DW stability is sometimes discussed in terms of a 'restoring pressure' [29], or a 'random pinning field' [30–32]. Hrianca [12] examined the motion of a 90° DW when activated by the stress. By establishing, in Becker's and Dörring's terms, the energetic conditions under which periodic torsion triggers forward and reverse Barkhausen jumps of such a DW in the presence of a magnetic field, he evaluated statistically the number of these local events and derived an expression for the amplitude and field dependence of the MMD. In the same view, Smith and Birchak [17] proposed a statistical model based on the concept of 'effective stress', by which the action of both the stress and magnetic field on the DWs are taken into account.

The influence of the dc magnetic field on the damping capacity of stress-relieved polycrystalline Ni is examined in the present paper under low frequency torsional vibrations in free decay; a strong effect of the field was detected. To some extent, our MMD data are consistent with the predictions of both Hrianca's and Smith's and Birchack's models, but aiming at a better description of the observed facts a new approach, in which some assumptions used by Hrianca were adopted in an equivalent form, is proposed. An attempt to evaluate the overall energy loss ΔW_m by adding contributions from cyclic processes consisting of vibration-triggered forward and reverse Barkhausen jumps of the non-180° DWs is now made, and in this view an expression for the amount δW_m of energy dissipated during such a local process is derived. Earlier versions of the model (not including this latter feature) were discussed elsewhere [33, 34].

2. Experiment

Magnetization and damping measurements were carried out on a 12 cm long cylindrical sample from a polycrystalline Ni layer of thickness $d = 45$ μm and radius $r = 0.6$ mm. The layer was electrodeposited on a Cu wire, using a Watts bath containing $NiSO_4$ and $NiCl_2$. In order to remove the inherent internal stresses, the sample was annealed for 2 h at 300 °C in silicon oil. Both measurements were performed via PC-assisted analog-to-digital conversion and data acquisition; a 12 bit resolution card (*NuDAQ-8112HG-ADLink Tech.*) was used.

The magnetic behaviour was examined under quasi-static conditions, in slowly varying (24 s period) triangular waveform longitudinal fields, by means of a conventional induction hysteresis graph using chopper-stabilized operational amplifiers (*ICL7650-Intersil*) for signal processing. The magnetic field was generated by a 30 cm long coil with a field uniformity better than 98% within ±10.5 cm from the midpoint. In figure 1 the magnetic behaviour of the sample in the as-deposited state and subsequent to annealing are shown: the drastic reduction in coercivity (from 11.4 kA m^{-1} to 127 A m^{-1}) confirms structural relaxation (via dislocation recovery and grain growth [35]) to a considerable extent.

An important increase in the damping capacity resulted from annealing, from MMD hardly separable from the non-magnetic background in the native state, to D_m values two orders of magnitude greater, now amplitude and field dependent. The IF was measured at frequencies close to 1 Hz under torsional vibrations in free decay, by means of an inverted pendulum using a tungsten wire, 0.1 mm in diameter, as elastic suspension. The angular deflection of the pendulum

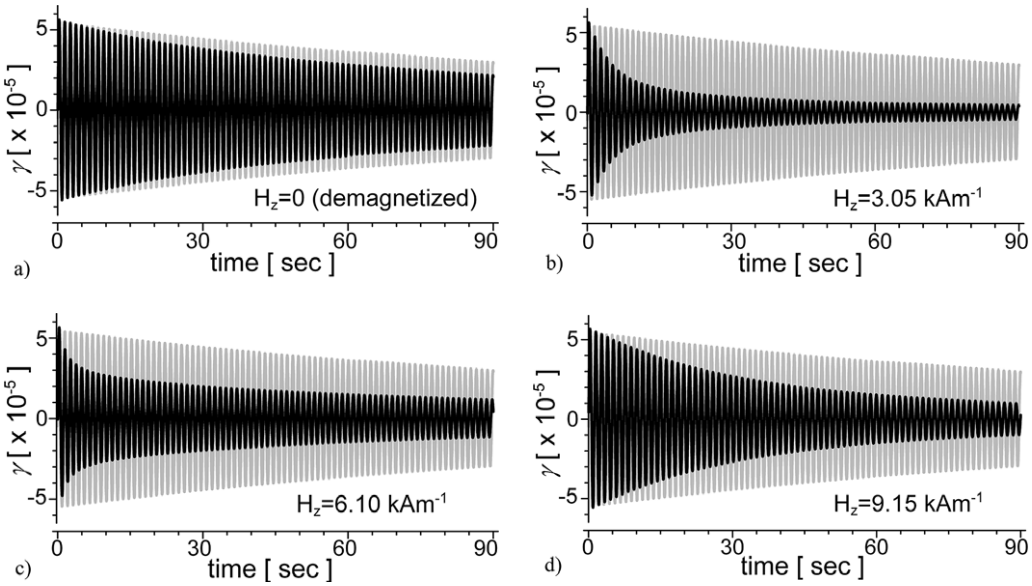

Figure 2. Sequences from torsional vibration records at constant longitudinal dc magnetic field H_z, increasing from (a) to (d); the sample is in the annealed state. The grey background is the vibrogram recorded at technical saturation (in a field $H_z = 30.2$ kA m^{-1}).

was converted into a voltage by means of a Hall effect-based transducer with a resolution better than 6×10^{-4} rad; details are given elsewhere [36]. During vibrations a dc magnetic field was applied longitudinally in equal steps of 508 A m^{-1}; the field strength was maintained constant until motion extinction and then *in situ* ac demagnetization was performed prior to the next vibration initiation. Vibrograms were recorded as the time evolution of the torsional strain (γ) in the median shell of the layer; in figure 2 a synthetic picture, showing the strong effect of the magnetic field on the damping is given.

The damping capacity was evaluated within the conventional low-amplitude approximation $W_e \propto \Gamma^2$ (here, Γ is the amplitude of the strain), by full rectification of the as-recorded vibrogram envelopes. An apparent damping coefficient, D_a, including contributions from both the Ni layer and the substrate Cu wire primarily resulted (the small amount of energy stored in the elastic suspension wire, not exceeding 1% from W_e, was neglected). From the obtained family of curves $D_a(\Gamma)_{H_z}$, the amplitude dependence of D_m at constant field strength was evaluated as:

$$D_m(\Gamma)_{H_z} = k\left[D_a(\Gamma)_{H_z} - D_{a,sat}\right], \qquad (2.1)$$

where $D_{a,sat} \approx 1.6 \times 10^{-3}$ is the damping at magnetic saturation (found to be independent of the amplitude of vibration) and

$$k = 1 + \left[(G_{Ni}/G_{Cu})\,(1 + d/r)^4 - 1\right]^{-1} \qquad (2.2)$$

is a correction factor (the calculation gives $k = 2.64$) required by the fact that the denominator W_e in equation (1.2) should exclusively be the elastic energy stored in the Ni layer, and G_{Ni} and G_{Cu} are the shear moduli of the two metals. From sectioning the generated curves $D_m(\Gamma)_{H_z}$ the family of curves $D_m(H_z)_\Gamma$ was obtained; the results are plotted in figure 3.

As a general feature, D_m exhibits broad maxima versus H_z, which is commonly expected. Less common is the fact that

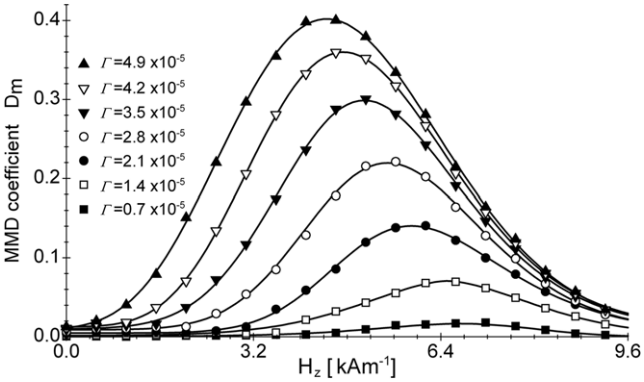

Figure 3. Magnetic field dependence of the MMD as exhibited by the sample in the stress-relieved state at different values of the amplitude of vibration (the interpolation lines are eye guides). The field was applied along the longitudinal axis.

the observed damping maxima are considerably high, reaching 40% fractional energy loss per full period. As the amplitude of vibration increases, these maxima progressively increase (the explored range of maximum strain was limited to the ascending side of the amplitude dependence of the MMD) and shift towards lower values of the field strength. In weak fields the MMD coefficient is very small, comparable to D_{sat} in order of magnitude.

3. Discussion

When compared to other data reported on polycrystalline Ni wires [4, 12], the shift of the D_m maxima is somewhat more evident, presumably due to the fact that the vibrational strain is practically uniform throughout the cross section of our relatively thin-walled sample. Vanishing MMD as detected in weak fields was also reported with annealed low carbon

steel [4]; substantial internal stress relief was achieved in both cases. In addition, it follows from figure 3 that the major damping effects occur in fields that drive the sample beyond 90% from technical saturation, as the examined quasi-static magnetic behaviour shows.

3.1. The field required for maximum damping

The fact that the maximum MMD requires high magnetization is neither singular, nor restricted to Ni [13, 22, 37]. According to the standard picture of the bulk magnetization process, in the field range of high magnetization the DW movements have already been completed [25b, 27c], which suggests that ferromagnets approaching technical saturation tend, if not to a single domain stage, (which is the case of small crystals like grains, thin films, whiskers), at least to a configuration consisting in a limited number of large volumes aligned (or close) to the field direction [38]. Correspondingly, most of the DWs must have vanished by this stage, and as far as the MMD is attributed to the MMH, the observed high field positions of the maximum damping do not appear as expected. Yet, this may have a simple explanation if we assume that in such stages of high magnetization there still exist some 'non-aligned islands' divided into domains inside which the dipoles point in directions other than parallel to the field, but energetically equivalent (quasi-equivalent), which makes the separating DWs practically insensitive to the field. Such equivalent directions may be either normal to the field, or other than normal, but symmetric (quasi-symmetric) with respect to this; 180° DWs are expected in the former case (which, clearly, is improbable in the high magnetization stages) and non-180° DWs in the latter. But if the material is magnetostrictive, the above orientational equivalence will be affected inside the domains separated by non-180° DWs, if a stress is applied along a direction which is other than parallel or normal to the field. Indeed, such a stress will cause changes of different amounts in the energy of the dipoles from the two sides of these walls and, consequently, those domains in which the dipoles' energy decreases will tend to expand at the expense of their less favoured neighbours. In other words, some non-180° DWs still existing in stages of high magnetization are almost insensitive to the field, but they may be sensitive to the stress if it is suitably applied. When referring to our Ni layer, such DWs are expected to be either transverse (quasi-transverse) or parallel (quasi-parallel) to the cylinder axis; from magnetostatic reasons, the magnetization component normal to the DW is continuous across the wall in the former case, and zero in the latter [27b]. Once the sample is driven into such a configuration by a dc field and then subjected to torsion, the energy of the dipoles from the two sides of these DWs will change and, since the local equivalent of torsion is shear, having tension and compression acting in quadrature as principal stress components, these changes will be close in value but opposite in sign. As a consequence, the DWs will change their position of equilibrium, and inside the as-swept volume the transverse component of the magnetization will change sign. The motion of the DWs will be forth and back if the torsion is periodic and, as far as Barkhausen jumps are concerned, energy dissipation will be produced. Evidence of such a mechanically-driven motion of the non-180° DW has been reported as the 'dynamic Matteucci effect' [40] with a Ni layer of shape and thermal history similar to ours': when a longitudinal dc magnetic field was applied during forced torsional vibrations, an ac voltage having the same period as the strain was detected across its ends. As the amplitude of the strain was increased, the amplitude of the signal also increased and gradually changed waveform from sine-like to narrow alternating pulses. Like in our damping experiment, the maximum effect required relatively strong fields, nearly exceeding the field range in which the conventional Barkhausen effect was detected (as well known, it is the irreversible movement of the DWs, mostly of 180° type, that has the dominant contribution to the steep part of the magnetization curve or of the hysteresis loop branches). Again like in our experiment, the field position of the maximum effect shifted towards lower values as the amplitude of the vibrations was increased. Clearly, the 'Matteucci voltage' was induced by the circular magnetic flux reversals, as a cumulative effect of the transverse component reversals of the dipoles moments, inside the volumes swept by some non-180° DWs, moving under the action of the periodic torsion. As the amplitude of the strain was increased, the character of this movement changed from reversible to irreversible, the signal increased in amplitude and its waveform turned into a succession of envelopes of the induced alternating Barkhausen avalanches.

3.2. Theory

In order to draw a somewhat more definite picture of the observed effect of the magnetic field on the damping, consider first a non-180° DW, moving through a magnetostrictive ferromagnet containing structure defects. Let ξ be the DW abscissa along the local direction of motion (assumed normal to the wall) and let $U(\xi)$ be the potential function associated with its interaction with the structure defects. Since these defects are distributed at random, the potential function is expected to exhibit a random profile. In the absence of any external forces, the DW positions of stable (metastable) equilibrium correspond to the local minima of $U(\xi)$, and if the wall eventually leaves such a position, a 'restoring force':

$$F_r(\xi) = -\langle \mathrm{d}U/\mathrm{d}\xi \rangle_w \tag{3.1}$$

will drive it back; here, $\langle \cdots \rangle_w$ denotes mediation over the DW thickness, which will be assumed small compared to the distance between two successive minima of $U(\xi)$. The stable equilibrium conditions $F_r(\xi) = 0$; $\mathrm{d}F_r/\mathrm{d}\xi < 0$, will be altered if external forces (e.g. a magnetic field or a stress) are applied, and the DW will move until their effect is counterbalanced by the generated restoring force; depending on both the direction and magnitude of these forces and, also, on the pinning field profile described by $F_r(\xi)$, the motion may be either reversible or irreversible.

However, since the DW is a topological object (a transition zone of magnetic moments rotation) rather than a moving body, it is more likely that its stability should be related to the coupling between the magnetic dipoles and the internal stress

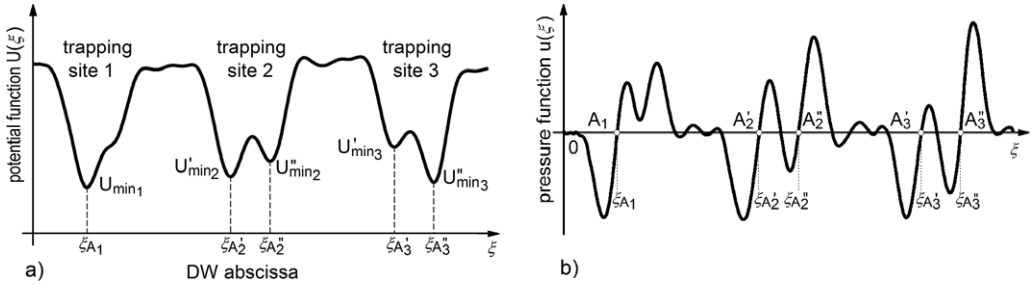

Figure 4. Plots of the potential function describing the interaction of a non-180° DW with the structure defects (a) and of the corresponding pressure function (b).

pattern generated by the structure defects. In this sense, we note that the stable positions of the DW will be those in which neither of the dipoles' orientations in the adjacent domains is energetically preferred [7b]; indeed, any eventual displacement from such a position will cause an increase of energy inside the as-swept volume. This suggests that the required conditions for the stability of the DW may be examined in terms of the difference [7b, 25a]:

$$u(\xi) = w^{\mathrm{b}}_{\mathrm{int}}(\xi) - w^{\mathrm{f}}_{\mathrm{int}}(\xi), \tag{3.2}$$

between the contributions $w^{\mathrm{b}}_{\mathrm{int}}(\xi)$, and $w^{\mathrm{f}}_{\mathrm{int}}(\xi)$, of internal origin to the energy density of the magnetic dipoles, as they belong to the domain behind the wall and to that in front of the wall, respectively. Since the anisotropy energy is the same in both domains, these contributions are primarily attributed to the internal stresses. In these terms, the DW positions of stable equilibrium in the absence of any external forces will correspond to the following conditions:

$$u(\xi) = 0; \qquad \mathrm{d}u/\mathrm{d}\xi > 0. \tag{3.3}$$

Clearly, a generic correspondence may be established between the two functions, $U(\xi)$ and $u(\xi)$. Indeed, the latter may be regarded as a direct measure of the 'external pressure' required to maintain a non-180° DW in equilibrium at position ξ, against the restoring pressure $F_{\mathrm{r}}(\xi)/A_{\mathrm{w}}$ (here, A_{w} is the area of the wall). Accordingly, we may write:

$$u(\xi) = A_{\mathrm{w}}^{-1}\langle \mathrm{d}U/\mathrm{d}\xi\rangle_{\mathrm{w}}. \tag{3.4}$$

Possible profiles of the potential function and of the derived 'pressure function', similar to those considered in [27a, 41, 42] are shown in figure 4; here, at points like A_1, A_2', A_2'', A_3', A_3'', etc, conditions (3.3) hold.

If a stress $\boldsymbol{\sigma}$ and a magnetic field $\boldsymbol{H}$ are applied along directions other than parallel or normal to the bisectrix of the DW angle, the generated contributions $w^{\mathrm{b}}_{\mathrm{ext}}(\xi, \boldsymbol{\sigma}, \boldsymbol{H})$ and $w^{\mathrm{f}}_{\mathrm{ext}}(\xi, \boldsymbol{\sigma}, \boldsymbol{H})$ to the energy density of the magnetic dipoles will differ from each other. Accordingly, the conditions for the stable equilibrium of the DW will be rewritten as:

$$\Delta w\,(\xi, \boldsymbol{\sigma}, \boldsymbol{H}) = 0; \qquad \partial \Delta w/\partial \xi > 0, \tag{3.5}$$

where

$$\Delta w\,(\xi, \boldsymbol{\sigma}, \boldsymbol{H}) = \left[w^{\mathrm{b}}_{\mathrm{int}}(\xi) + w^{\mathrm{b}}_{\mathrm{ext}}\,(\xi, \boldsymbol{\sigma}, \boldsymbol{H})\right] - \left[w^{\mathrm{f}}_{\mathrm{int}}(\xi) + w^{\mathrm{f}}_{\mathrm{ext}}(\xi, \boldsymbol{\sigma}, \boldsymbol{H})\right]. \tag{3.6}$$

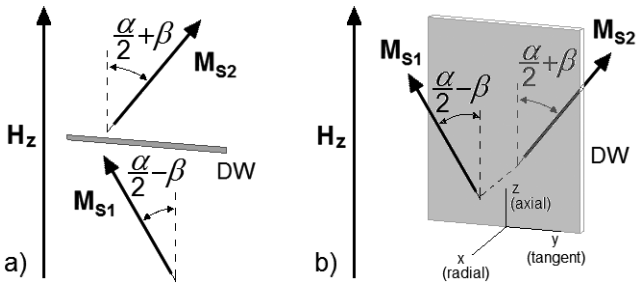

Figure 5. Possible orientations of non-180° DWs in strong longitudinal fields H_z: (a) quasi-transverse, (b) longitudinal.

In particular, if the ferromagnet is (like our Ni sample) a hollow cylinder of thickness small compared to the radius, the applied torsion will produce a strain (γ) which is practically uniform, and if a solenoid-type coil is used to generate a longitudinal magnetic field H_z, this will also be uniform. Accordingly, conditions (3.5) take the simple form:

$$u(\xi) = c_\gamma \gamma + c_z H_z; \qquad \mathrm{d}u/\mathrm{d}\xi > 0 \tag{3.7}$$

where coefficients c_γ and c_z depend on the material constants and magnetic dipoles orientations. If α is the DW angle and $\mp\beta$ are the deviations of the M_{S} vectors from the symmetric $\pm\alpha/2$ directions with respect to the field in the adjacent domains (figure 5), these coefficients are:

$$c_\gamma = -3\lambda G \sin\alpha \cos(2\beta); \qquad c_z = 2\mu_0 M_{\mathrm{S}} \sin(\alpha/2) \sin\beta, \tag{3.8}$$

where λ is the magnetostriction constant, G is the shear modulus and μ_0 is the vacuum permeability.

As far as concerns our Ni sample, the axes of easy magnetization belong to the $\langle 111\rangle$ family of crystal directions, which means that the DW angle α is either 70° 30′ or 109° 30′, but for energetic reasons a DW of the latter type is significantly less probable than the former in the H_z range favouring high MMD. Accordingly, we shall ignore the blunt angle DWs in what follows.

In addition, it is known that Ni exhibits negative magnetostriction. Then, if α and β are considered positive quantities, both $c_\gamma > 0$ and $c_z > 0$ (note that $c_\gamma < 0$ corresponds to $\beta > 45°$, a value also unlikely in the field range of interest). For convenience, we shall complete this sign convention by associating $\gamma > 0$ with clockwise torsion and $H_z > 0$ to the DW moving towards an increasing abscissa.

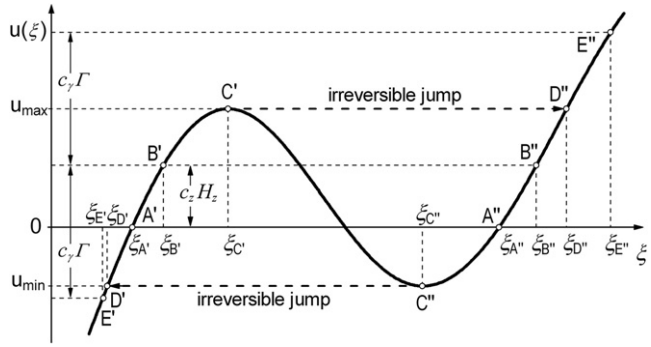

Figure 6. The path of the representative point associated with the motion of a non-180° DW inside the trapping site 2 in figure 4 (the index 2 was omitted for simplicity).

It is common practice [25a, 27, 41, 42] to discuss the movement of the DW through the real crystal in direct relation with that of a point (the 'representative point') along the position-dependent graph of the DW energy or energy gradient. Following Becker's description [7b], also used by Hrianca [12], this may be done in our terms by examining the motion of the representative point on the graph of the pressure function $u(\xi)$. Depending on the combined effect of the applied field and stress, this point either moves reversibly along an ascending graph side, or jumps from an as-reached extremum to the nearest accessible side; an illustration is given in figure 6, in which a DW captured in the trapping site 2 in figure 4 is assumed.

Let, in the absence of any external forces, the DW in stable equilibrium be in position $\xi_{A'}$ (the representative point in A'). If a dc magnetic field of strength $0 < H_z < c_z^{-1}u(\xi_{C'})$ is now applied, the DW moves to, say, $\xi_{B'}$ (the representative point shifts from A' to B', on the same side of the graph) and if periodic torsion is superimposed, the DW begins to move back and forth about this new position of equilibrium. Depending on the amplitude of the strain, the motion will be either reversible or irreversible. In terms of the local extrema $u_{\max} = u(\xi_{C'})$ and $u_{\min} = u(\xi_{C''})$ of the pressure function $u(\xi)$, the path of the DW is a short segment about position $\xi_{B'}$ (the representative point moves reversibly up and down about point B') if the amplitude Γ of the strain is less than

$$\gamma_{(\mathrm{rev})} = c_\gamma^{-1} \min\{c_zH_z - u_{\min}, u_{\max} - c_zH_z\}, \qquad (3.9a)$$

but it extends considerably (say, between $\xi_{E'}$ and $\xi_{E''}$) if the amplitude is increased beyond

$$\gamma_{(\mathrm{irr})} = c_\gamma^{-1} \max\{c_zH_z - u_{\min}, u_{\max} - c_zH_z\}. \qquad (3.9b)$$

The extension is primarily due to the forward ($\xi_{C'} \to \xi_{D''}$) and reverse ($\xi_{C''} \to \xi_{D'}$) Barkhausen jumps now triggered (the representative point follows the cyclic path $B' \to C' \to D'' \to E'' \to B'' \to C'' \to E' \to B'$). The DW eventually performs one of these two jumps if $\gamma_{(\mathrm{rev})} < \Gamma < \gamma_{(\mathrm{irr})}$, then moving reversibly about one of the two zero-strain positions $\xi_{B'}$ and $\xi_{B''}$; clearly, an effective contribution to the damping requires $\Gamma > \gamma_{(\mathrm{irr})}$.

In order to express the energetic conditions according to which a cyclic dissipative process runs under given field and amplitude conditions, we shall use the positive quantities introduced by Hrianca [12]:

$$\varphi = u_{\max}; \qquad \psi = u_{\max} - u_{\min} \qquad (3.10a)$$

and:

$$\rho = c_\gamma\Gamma; \qquad \eta_z = c_zH_z, \qquad (3.10b)$$

as 'internal' and 'external' variables, respectively. In these terms, the above conditions are:

$$\eta_z \leqslant \varphi \leqslant \rho + \eta_z; \qquad \psi - \varphi \leqslant \rho - \eta_z. \qquad (3.11)$$

During such a process an amount δW_m of energy will be dissipated, and this may be estimated as:

$$\delta W_m = \mathrm{A_w} \oint u(\xi)\,\mathrm{d}\xi, \qquad (3.12)$$

where the integration path is the contour $D' \to C' \to D'' \to C'' \to D'$, delimited by the endpoints of the two Barkhausen jumps. Approximating this contour to a trapezium, the calculation yields:

$$\delta W_m \approx \kappa \mathrm{A_w} \psi^2 \qquad (3.13)$$

where κ is a factor related to the profile of $u(\xi)$; in terms of the average slopes $s_{D'C'}$, $s_{C'C''}$ and $s_{C''D''}$ of the graph segments enclosed by the integration contour, $\kappa = 0.5/s_{D'C'} - 1/s_{C'C''} + 0.5/s_{C''D''}$.

In order to evaluate ΔW_m, we shall extend the calculus to the whole ferromagnet (in particular to our Ni layer) on the basis of the following general assumptions: (i) the local dissipative events activated by the torsional vibrations may be approximated by simple processes running in compliance with conditions of the form (3.11), and (ii) these processes are activated in a number which is large enough to treat ΔW_m as a statistical addition of their contributions δW_m.

To what extent assumption (i) holds remains an open question, but some arguments may still be put forward. Thus, on one hand, we shall note that in the explored range of moderate amplitudes of the vibrations, low D_m values were detected both in weak and in strong fields, which corresponds in our terms to $\eta_z \ll \rho$ and to $\eta_z \gg \rho$, respectively. Thus it is reasonable to expect that amplitude and field conditions favouring strong MMD correspond to variables η_z and ρ falling into the same order of magnitude, and the calculation shows that this requires small angles β, not exceeding a few degrees. In this sense, the following example is suggestive: given $G = G_{110} = 7.6 \times 10^{10}$ N m^{-2} [43], $\lambda_S = \lambda_{111} = 2.7 \times 10^{-5}$, $\mu_0 M_S = 0.61$ T [44] as material constants, and $\Gamma = 4.9 \times 10^{-5}$, $H_z = 4$ kA m^{-1} as experimental conditions leading to D_m close to the maximum detected, the ratio ρ/η_z ranging within reasonable limits, say, 1 and 3 (in figure 5 this ratio is close to 2), corresponds to $2° < \beta < 5°\ 30'$, in agreement with the previous interpretation (section 3.1) of the strong fields positions of the D_m maxima. Indeed, the MMD here is attributed to the irreversible jumps of the non-180° DWs separating some domains remaining

unaligned to the field, inside which the magnetization slightly deviates from the $\pm\alpha/2$ symmetric directions with respect to the field. On the other hand, if all the four variables, both internal (φ, ψ) and external (ρ, η_z), take comparable values in such a process (again, figure 5 is illustrative), the estimated order of magnitude of the internal stresses having generated restoring pressure peaks comparable with the local extrema of $u(\xi)$ is 10 MPa, which is the residual stress level reported in annealed Ni [4]. With regard to assumption (ii), if the MMD is due to such processes, their expected number (N_p) is of the order of 10^5 in our experiment, a number sufficiently large to make a statistical approach acceptable. This number results from comparing the amount $\delta W_{m,\mathrm{av}} \sim 10^{-11}$ J of energy dissipated in the course of an 'average process' with the overall loss per full period $\Delta W_m \sim 10^{-6}$ J evaluated in our sample in the range of high MMD. In defining the above average process, the following reasonable values were assumed: a DW $\sim$ 25 μm $\times$ 100 μm in size, performing $\sim$10 μm long Barkhausen jumps (thus, sweeping a volume $\delta V_{(\mathrm{irr}),\mathrm{av}} \sim 2.5\times10^{-14}$ m^3) inside a trapping site where a peak-to-peak fluctuation $\psi_{\mathrm{av}} \sim 400$ J m^{-3} in the restoring pressure was generated by a $\sim$10 MPa internal stress directed at 45° with respect to the normal to the wall; the total volume swept by the DWs per full period is then estimated as the product $N_p\delta V_{(\mathrm{irr}),\mathrm{av}}$. Clearly, as far as the major damping effects require stages of high magnetization, this volume should not exceed a small fraction of the volume of our Ni layer, and since the calculation leads to a value $\sim$3% for this fraction, the above-estimated N_p appears as a reasonable number. In addition, since sweeping out a magnetic domain is not the consequence of a single Barkhausen event, a somewhat larger value should correspond to the volume fraction of the non-aligned domains. Thus, if the volume fraction of these domains is, say $\sim$20% and if the separating DWs are like those in figure 5 (i.e. of 70° 30′ and quasi-transverse or longitudinal), the estimated bulk magnetization is $\sim$96% from saturation, a value in good agreement with experiment.

In agreement with assumptions (i) and (ii), a pair (φ, ψ) of internal variables will be associated with each of the existing trapping sites. Since $u(\xi)$ is a random profile function, these variables will be regarded as statistically independent and, expressing the space fluctuations of the same quantity, it is natural to expect that they obey similar distribution laws. Accordingly, the associated distribution functions $f(\varphi)$ and $f(\psi)$ will be assumed of the same analytic form (up to a scaling factor). In order to identify the processes contributing to the MMD, we shall take into account the fact that only a small number of trapping sites contain DWs, and also that a DW has to perform a certain number of Barkhausen jumps to completely sweep out a magnetic domain. In other words, the DW has to overcome a certain number of 'pinning barriers' while crossing, and a direct measure of the barrier heights is provided in our description by the local maxima of the pressure function $u(\xi)$. The higher such a barrier is, the more likely it will stop the moving DW, and in this sense, a probability function $p(\varphi)$, increasing with the argument, will be introduced as a measure of this stopping capability. Since trapping sites always contain barriers, $p(\varphi)$ may be regarded as expressing their expected 'degree of occupation'.

With these considerations, we shall evaluate ΔW_m by integrating elementary quantities of the form:

$$\mathrm{d}W_m(\varphi, \psi) = N_{\mathrm{w}}\delta W_m\, p(\varphi) f(\varphi) f(\psi)\, \mathrm{d}\psi\, \mathrm{d}\varphi, \qquad (3.14)$$

between the limits resulting from conditions (3.11); here N_{w} is the number of the walls. The calculation will be considerably simplified if the individual process-quantities A_{w} and κ are averaged to some 'effective values', $A_{w,\mathrm{eff}}$ and κ_{eff}, respectively. Adopting this approximation, we may write:

$$\Delta W_m(\rho, \eta_z) = N_{\mathrm{w}}\kappa_{\mathrm{eff}} A_{w,\mathrm{eff}} I(\rho, \eta_z) \qquad (3.15)$$

with

$$I(\rho, \eta_z) = \int_{\eta_z}^{\rho+\eta_z} p(\varphi) f(\varphi) \int_0^{\rho-\eta_z+\varphi} \psi^2 f(\psi)\, \mathrm{d}\psi\, \mathrm{d}\varphi. \qquad (3.16)$$

As long as variables ρ and η_z still depend (via coefficients c_γ and c_z) on α and β, integration will not automatically lead to the aimed amplitude and field dependence of the damping. In order to clarify the role of these two angles, we first note that as regards α, a decrease of only a few degrees from the original 70° 30′ value (via vector rotations) is expected in the H_z range related to significant MMD. It follows then from the first relation (3.8) that the coefficient c_γ remains almost constant, in which case ρ is a 'true' external variable. On the other hand, if β is restricted to small values, the second relation (3.8) reveals that a dispersion of several degrees of this angle will only affect the coefficient c_z by a factor of the order of unity. Then, if the influence of this factor is mediated over a numeric range of the same order of magnitude, i.e. if the double integral (3.16) is replaced with:

$$I_\varepsilon(\rho, \eta_z) = \frac{1}{\varepsilon}\int_{\eta_z}^{(1+\varepsilon)\eta_z} I(\rho, \tau)\, \mathrm{d}\tau; \qquad 0 \leqslant \varepsilon \leqslant 1, \quad (3.17)$$

within a reasonable approximation η_z may also be regarded as a true external variable.

Numeric evaluation of ΔW_m requires known values for N_{w}, $A_{w,\mathrm{eff}}$ and κ_{eff}, as well as known analytic forms for $p(\varphi)$, $f(\varphi)$, and $f(\psi)$, which involves full examination (or at least throughout a representative volume) of both the magnetic domain pattern and internal stress distribution. Since such a task is hardly possible, we shall limit our calculation to qualitative predictions, based on suitable analytic forms, consistent with the structural state of the sample, for the above functions. Accordingly, the remaining question is to what extent the ratio $I_\varepsilon(\rho, \eta_z)/\rho^2$ reproduces the dependence $D_m(\Gamma, H)$. Having this end in view, we recall the fact that the drastic reduction in coercivity subsequent to annealing provides a direct confirmation of a substantial structure defects relaxation in our Ni layer. It is, then, reasonable to expect that the more severe a still remaining defect is, the less probable it is, and keeping in mind the physical meaning of the pressure function $u(\xi)$, the internal variables φ and ψ should obey the same rule. Correspondingly, forms decreasing with the argument are expected for $f(\varphi)$ and $f(\psi)$, and in this sense we shall consider the Gaussian half normal [44]:

$$f(x) = 2\,(\pi\,\langle x\rangle)^{-1} \exp\left[-\left(\sqrt{\pi}\,\langle x\rangle\right)^{-2} x^2\right];$$
$$x = \varphi, \psi > 0 \qquad (3.18)$$

as a possible choice meeting this requirement; here, $\langle x\rangle$ is the mean.

Concerning the 'probability of occupation' $p(\varphi)$, we shall adopt the Gauss cumulative form:

$$p(\varphi) = 0.5\{1+\mathrm{erf}[\upsilon(\varphi/\varphi_0-1)]\}; \qquad \varphi, \varphi_0, \upsilon > 0 \quad (3.19)$$

where the scaling factor φ_0 corresponds to the height of a pinning barrier having a 50% chance to retain a DW. Clearly, a reasonable value of the shape factor υ should correspond to a vanishing probability of occupation at $\varphi = 0$, a condition satisfactorily fulfilled for, say $\upsilon > 2$; indeed, $\upsilon = 2$ leads to $p(0) = 0.0023$, $\upsilon = 3$ to $p(0) = 1.1 \times 10^{-5}$, $\upsilon = 4$ to $p(0) = 7.7 \times 10^{-9}$, etc.

A numerical calculation based on the analytic forms (3.18) and (3.19) still requires known values for the means $\langle\varphi\rangle$ and $\langle\psi\rangle$, as well as known ranges for variables φ, ψ, η_z and ρ. The difficulty is avoided by introducing some dimensionless variables, and a convenient way to make the substitution is provided by the fact that, as definition (3.10*a*) suggest, the following relation:

$$\langle\psi\rangle = 2\langle\varphi\rangle \quad (3.20)$$

should hold. Accordingly, we shall introduce the new ('reduced') variables as:

$$\varsigma = \varphi/(\sqrt{\pi}\langle\psi\rangle); \qquad \zeta = \psi/(\sqrt{\pi}\langle\psi\rangle) \quad (3.21)$$

and:

$$g = \rho/(\sqrt{\pi}\langle\psi\rangle); \qquad h_z = \eta_z/(\sqrt{\pi}\langle\psi\rangle), \quad (3.22)$$

In these terms, the distribution functions (3.18) and the probability of occupation (3.19) take the form:

$$f(\varsigma) = (4/\sqrt{\pi})\exp(-4\varsigma^2); \qquad f(\zeta) = (2/\sqrt{\pi})\exp(-\zeta^2); \qquad \varsigma, \zeta > 0 \quad (3.23)$$

and

$$p(\varsigma) = 0.5\{1 + \mathrm{erf}[\upsilon(\varsigma/\varsigma_0 - 1)]\}; \qquad \varsigma_0, \varsigma, \upsilon > 0, \quad (3.24)$$

where ς_0 is the correspondent of φ_0. Consequently, integrals (3.16) and (3.17) will be rewritten as:

$$I(g, h_z) = \int_{h_z}^{g+h_z} p(\varsigma) f(\varsigma) \int_0^{g-h_z+u} \zeta^2 f(\zeta)\, \mathrm{d}\zeta\, \mathrm{d}\varsigma, \quad (3.25)$$

and

$$I_\varepsilon(g, h_z) = \varepsilon^{-1} \int_{h_z}^{(1+\varepsilon)h_z} I(g, q)\, \mathrm{d}q; \qquad 0 \leqslant \varepsilon \leqslant 1. \quad (3.26)$$

With these considerations, we shall regard $d_m(g, h_z) = g^{-2} I_\varepsilon(g, h_z)$ as a representation of $D_m(\Gamma, H_z)$. In this sense, an example is given in figure 7, in which the family of curves $d_m(h_z)_g$ are plotted using the set of parameters: $\upsilon = 9/2$, $\varsigma_0 = 3/2$ and $\varepsilon = 1/2$.

When these curves are compared with the family of experimental curves $D_m(H_z)_\Gamma$ in figure 3, a good similarity may be observed. But apart from this 'graphical' agreement, additional arguments supporting the validity of the model may be put forward. Thus, the choice for the set of parameters used in the calculation of the theoretical curves is justified as follows: $\varepsilon = 1/2$ corresponds to a dispersion of the DW orientations within reasonable limits ($3° \leqslant \beta \leqslant 4°\ 30'$) and $\varsigma_0 = 3/2$ to $\varphi_0 = 3\sqrt{\pi}\langle\varphi\rangle$. The latter value is consistent with a limited population of the pinning barriers; indeed, this implies $\varphi_0 > \langle\varphi\rangle$, but not $\varphi_0 \gg \langle\varphi\rangle$, since the latter condition 'sends' the non-180° DWs towards such high barriers over which vibrations of moderate amplitudes, as in our experiment, could hardly activate Barkhausen jumps. As concerns the shape factor υ, the value $9/2$ corresponds to a probability of occupation showing a reasonable rise, from 1.7% for $\varsigma = 1$, to 98% for $\varsigma = 2$. In addition, if the ratio $c_\gamma \Gamma_{\max}/c_z H_{z,\max}$ is evaluated using values close to the original DW angle for α (i.e. 70° 30′), small angles β and amplitude and field ranges like those in figure 3, this should match the ratio $g_{\max}/h_{z,\max} \approx 0.52$ as results from figure 7: within reasonable approximation this condition is fulfilled (e.g. for $\beta = 4°$, $\Gamma_{\max} = 4.9 \times 10^{-5}$ and $H_{z,\max} = 9.6$ kA m^{-1}, one finds $c_\gamma \Gamma_{\max}/c_z H_{z,\max} \approx 0.59$).

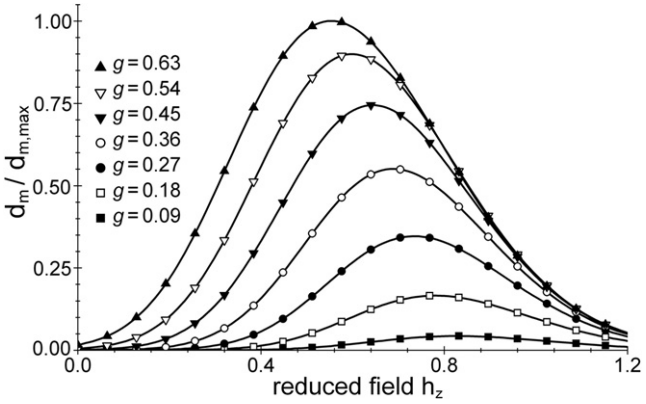

Figure 7. Predicted MMD dependence on the dc magnetic field at constant amplitude of vibration; the values of d_m are given in relative units ($d_m/d_{m,\max}$).

4. Conclusions

The influence of the dc magnetic field on the magnetomechanical damping in a stress-relieved cylindrical layer of polycrystalline Ni was examined under low frequency torsional vibrations in free decay. High damping, reaching 40% fractional energy dissipation per full period, was detected in stages of high magnetization, approaching 90% from technical saturation. The effect is attributed to the forward and reverse Barkhausen jumps (either favoured or inhibited by the field, depending on its strength) of some non-180° DWs, as they move, under the action of the vibrational stress, through the irregular energy landscape generated by their interaction with the still existing structure defects. This energy landscape is described by a DW position-dependent, random profile potential function $U(\xi)$, from which a restoring force $F_r(\xi)$, acting on the DW when leaving its equilibrium position, is derived.

The difference $u(\xi)$ between the energy densities of the magnetic dipoles from the two sides of the wall is regarded as a direct measure of the external pressure exerted by a magnetic field or a stress (or by both) against the restoring pressure, $F_r(\xi)/A_w$, required to maintain a DW of area A_w in a given position, other than of non-perturbed stable equilibrium. The conditions under which a non-180° DW performs forward and reverse Barkhausen jumps activated by the periodic torsion in the presence of a dc magnetic field are derived in terms of the local extrema of $u(\xi)$. An expression is derived in these terms for the energy δW_m dissipated in such a cyclic process, and the overall loss per full period ΔW_m is then evaluated as an addition of such contributions. In this view, statistically distributed space fluctuations of $u(\xi)$ are assumed and a probability of occupation is introduced in order to account for the way in which the trapping sites existing in the energy landscape are populated with DWs. Considering analytic forms consistent with the structural state of the sample for the distribution and probability functions, qualitative predictions in good agreement with the experimental results were obtained.

References

[1] Nowick A S and Berry B S 1972 *An Elastic Relaxation in Crystalline Solids* ed A M Alper, J L Margrave and A S Nowick (New York: Academic)
[2] Nowick A S and Berry B S 2001 *Mechanical Spectroscopy Q-1 2001 With Applications to Materials Science* ed R Schaller *et al* (Switzerland: Trans Tech Publ)
[3] Frank R C and Ferman J W 1965 *J. Appl. Phys.* **36** 2235
[4] Adams R D 1972 *J. Phys. D: Appl. Phys.* **5** 1877
[5] Coronel V F and Beshers D N 1988 *J. Appl. Phys.* **64** 2006
[6] Cochardt A W 1959 *Magnetic Properties of Metals and Alloys* ed R M Bozorth (Materials Park, OH: ASM International) p 251
[7a] Becker R and Döring W 1939 *Ferromagnetismus* (Berlin: Springer) p 365
[7b] Becker R and Döring W 1939 *Ferromagnetismus* (Berlin: Springer) p 150
[8] Kardashev B K, van Ouytsel K and de Batist R 2000 *J. Alloys. Compounds* **310** 169
[9] Becker R and Kornetzki M 1934 *Z. Phys.* **88** 634
[10] Kornetzky M 1956 *Z. Phys.* **146** 107
Kornetzky M 1948 *Ann. Phys.* **2** 265
[11] Frank R C and Swanson P A 1967 *J. Appl. Phys.* **38** 4549
[12] Hrianca I 1966 *Ann. Phys., Lpz.* **7** 233
[13] Cochardt A W 1954 *J. Appl. Phys.* **23** 670
[14] Good N and Dooley J 2002 *J. Appl. Phys.* **91** 7824
[15] Kronmüller H 1981 *J. Magn. Magn. Mater.* **24** 159
[16] Oelmann A 1975 *Physica* B+C **1–4** 95
[17] Smith G W and Birchak J R 1968 *J. Appl. Phys.* **39** 2311
Smith G W and Birchak J R 1969 *J. Appl. Phys.* **40** 5174
Smith G W and Birchak J R 1970 *J. Appl. Phys.* **41** 3315
[18] Williams H J, Bozorth R M and Christensen H 1941 *Phys. Rev.* **59** 1005
[19] Aczel O F G 1971 *Phys. Status Solidi* b **45** 253
[20] Birchak J R and Smith G W 1972 *J. Appl. Phys.* **43** 1238
[21] Shin D W, Degauque J and Astié B 2000 *J. Magn. Magn. Mater.* **215/216** 165
[22] Sumner G and Entwistle K M 1959 *J. Iron Steel Inst.* **192** 238
[23] Degauque J 2001 *Mechanical Spectroscopy Q-1 2001 with Applications to Materials Science* ed R Schaller *et al* (Switzerland: Trans Tech Publ) p 453
[24] Porteseil J L 1979 *Phys. Status Solidi* a **51** 107
[25a] Bates L F 1961 *Modern Magnetism* 4th edn (Cambridge: University Press) p 470
[25b] Bates L F 1961 *Modern Magnetism* 4th edn (Cambridge: University Press) p 472
[26] Néel L 1942 *Cahiers Phys.* **12** 1
Néel L 1943 *Cahiers Phys.* **13** 1
[27a] Chikazumi S 1963 *Physics of Magnetism* (New York: Wiley) p 286
[27b] Chikazumi S 1963 *Physics of Magnetism* (New York: Wiley) p 199
[27c] Chikazumi S 1963 *Physics of Magnetism* (New York: Wiley) p 246
[28] Kleman M 1982 *Magnetism of Metals and Alloys* ed M Cyrot (Amsterdam: North-Holland) p 516
[29] Tahara V and Sugeno T 1973 *Phys. Status Solidi* b **55** 385
[30] Bertotti G, Basso V and Durin G 1996 *J. Appl. Phys.* **79** 5764
[31] Mills A C, Hess F M and Weissman M B 2002 *Phys. Rev.* B **66** 140409(R)
[32] Dante L, Durin G, Magni A and Zapperi A 2002 *Phys. Rev.* B **65** 144441
[33] Ercuta A and Mihalca I 2002 *Deffect Diffus. Forum* **203–205** 269
[34] Ercuta A, Mihalca I, Chiriac H and Borza F 2002 *J. Opt. Adv. Mater.* **4** 361
[35] Lloyd J C and Smith R S 1962 *Can. J. Phys.* **40** 454
[36] Ercuta A and Mihalca I 2002 *J. Phys. D: Appl. Phys.* **35** 2902
[37] Atalay S and Squire P T 1991 *J. Magn. Magn. Mater.* **101** 47
[38] Beatrice C, Fiorillo F, Asti G, Solzi M and Sarzi Sartori S 2003 *J. Magn. Magn. Mater.* **254/255** 149
[39] Rothenstein B F and Policec A 1965 *J. Appl. Phys.* **36** 1808
[40] Kneller E 1962 *Ferromagnetismus* (Berlin: Springer) p 366
[41] Mayergoyz I D 2003 *Mathematical Models of Hysteresis and Their Applications* (Amsterdam: Elsevier) p 295
[42] Kikuchi Y 1969 *Ultrasonic Transducers* ed Y Kikuchi (Tokyo: Corona) p 49
[43] Bozorth R M 1959 *Ferromagnetism* (Princeton, NJ: Van Nostrand) p 270
[44] McMichael R D, Swartzendruber L J and Bennet L H 1996 *J. Appl. Phys.* **73** 5848